Design of Catadioptric Lens with Servo Optical Mechanism in Holographic Recording System

2008 Jpn. J. Appl. Phys. 47 5794

(http://iopscience.iop.org/1347-4065/47/7S1/5794)

Japanese Journal of Applied Physics
Vol. 47, No. 7, 2008, pp. 5794–5796

Communication

Design of Catadioptric Lens with Servo Optical Mechanism in Holographic Recording System

Yung-Sung LAN[1,2] and Chung-Hao TIEN[3]

[1]*Department of Photonics and Institute of Electro-Optical Engineering, National Chiao Tung University, Hsinchu 310, Taiwan*
[2]*Electronics and Optoelectronics Research Laboratories, ITRI, Hsinchu 310, Taiwan*
[3]*Department of Photonics and Display Institute, National Chiao Tung University, Hsinchu 310, Taiwan*

(Received December 5, 2007; accepted January 26, 2008; published online July 18, 2008)

In this paper, we present a catadioptric telecentric objective for a holographic recording system. The lens was made of Zeonex, whose aspherical surfaces were formed by diamond-turning machining. A least-squares method was used to solve a set of linear equations for the spot size of charge-coupled device (CCD). The data were obtained to generate an S curve, which was used in the pupil obscuration method, for the control of the system operated in a linear range of ±0.3 mm.
[DOI: 10.1143/JJAP.47.5794]

KEYWORDS: holographic recording, optical recording

An optical data storage (ODS) system can be divided into two approaches based on the way how data is recorded and readout: either by the format of bit (two-dimensional) or page (three-dimensional). Some unique advantages of holographic storage are extremely short access time, e.g., less than 50 s, extremely high input and output rates, more than 10 Gbit/s, enormous search capabilities for finding unaddressed information in databases at rates exceeding 100 Gbit/s, and therefore, much superior to current optical disk-based storage systems.[1)]

While multiple holograms are required to be superimposed, media must have excellent volumetric stability, low scatter, and high sensitivity for recording. Furthermore, as the superposition of holograms reduces the intensity of the reconstructed data pages owing to a high page density in the same volume, the sensitivity of the detector shall be sufficiently high for improving the signal-to-noise ratio. A 1024×1024 1000-fps digital Kodak C7 charge-coupled device (CCD) camera and a 1024×1024 2000-fps IBM FLC spatial light modulator (SLM) with a nearly 100% fill factor were used.[2)]

Typical optomechanical solutions can be divided into three types of design: finite/finite conjugate, infinite/infinite conjugate, and infinite/finite conjugate. In a finite/finite conjugate design, light from a source at a distance is focused to a corresponding point. Most imaging lenses are designed using this scenario, in which the camera lenses image the object at a finite distance onto a CCD sensor. In an infinite/infinite conjugate design, both object and image sides have telecentric structures often referred to as doubly telecentric or afocal lenses. The design uses a large number of lens elements; however, if is adequate for precise measurement applications, where the positions of both the camera and the inspected part must be rigorously defined. In an infinite/finite conjugate design, either object or image side has a telecentric structure for focusing light from a source at infinity down to a small spot and *vice versa*. Some compact disc objective lenses are designed using this scenario to focus the collimated light onto a disc at a finite distance.

The operation of Fourier transform is normally used in the signal path of a holographic system. One of the most remarkable and useful properties of a converging lens is its inherent ability to perform two-dimensional Fourier transform in a monochromatic system. According to the Abbe theory, only a certain portion of the diffracted light generated by a complex object is intercepted by a finite pupil. The light not intercepted is precisely that generated by the high-frequency components of the object amplitude transmittance. In general, for a diffraction-limited system, we can regard the image as a convolution of the image predicted by geometrical optics with an impulse response, which is the Fraunhofer diffraction pattern of the exit pupil.[3)]

Using the aforementioned concepts, two subsystems are described below.

(1) Recording/reproduction system

The strehl ratio of a catadioptric lens is calculated for optimization in Fig. 1. When the stop of the system is at the front focal plane, the exit pupil is at infinity and the small displacement of the image plane does not affect the image height. The working wavelength is $\lambda = 532$ nm. The mirror surfaces (a) and (b) are aspheric surfaces with the conic constants $K_{\mathrm{lens1}} = -1.73$ and $K_{\mathrm{lens2}} = -2.351$, respectively, as shown in Fig. 2. A system can bring light to a diffraction limited airy disc. The SLM has a resolution of 1024×768 in $1.5 \times 1.2\,\mathrm{mm}^2$. The design of a catadioptric lens to be a $4f$ Fourier configuration is due to the large field involved. However, the pixel size of the SLM that needs to be resolved at the detector array is much larger than the wavelength of light λ. This indicates that light from an individual pixel of the SLM is only diffracted into a small cone with $\mathrm{NA} = 0.01$. This system uses the reproduction method for phase conjugate readout, in which a reproduction reference beam propagates in a direction opposite to that of recording reference plane beam.

A two-mirror afocal system is a device for expanding a laser beam.[4)] A mirror element has several advantages over a refracting element. It is completely achromatic, having neither axial nor lateral color, nor chromatic variations of aberrations (e.g., spherochromatism). A third advantage is that the aberrations of a spherical mirror are inherently smaller than those of a comparable spherical lens. The third order of any two-mirror system can readily be determined. Given the focal length F, the back focus B, and the mirror spacing D, one can determine the required mirror curvatures for any configuration form, as expressed by[5,6)]

$$C_1 = \frac{B - F}{2DF} \quad \text{and} \quad C_2 = \frac{B + D - F}{2DB}.$$

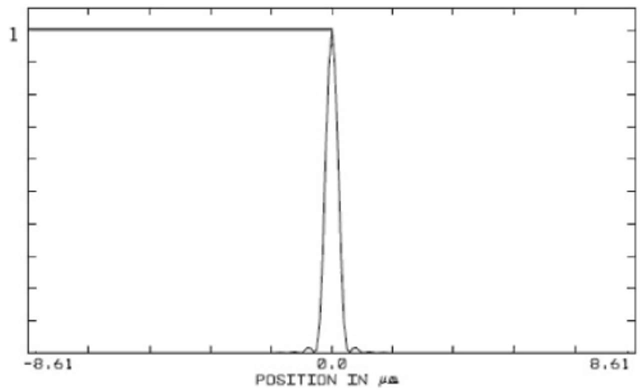

Fig. 1. Strehl ratio of catadioptric lens.

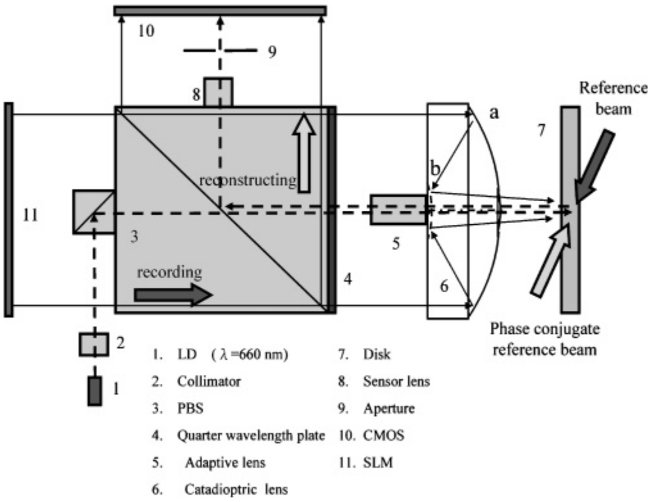

Fig. 2. Entire system layout.

The fundamental philosophy behind most catadioptric systems is the use of refracting elements to correct the aberrations of a system. In this system, the third surface is added of the end of the catadioptric system to allow aberration correction. Therefore, the conic constants and aspheric order terms can be optimized using the optical simulation tool ZEMAX™.

(2) Servo system

The laser diode ($\lambda_{\rm SERVO} = 660$ nm) is applied as the source of the servo system, as shown in Fig. 2. The laser diode emits a beam, which goes through the two PBS cubes, wave plate, adaptive lens and cassegrain lens, and is finally focused on the disc. Subsequently, the servo beam is reflected back to the central area of the CCD sensor, which has a resolution of 1280×1024 in $1.4 \times 1.2\,\text{mm}^2$. The pupil obscuration method shown in Fig. 3 has the advantage of a high degree of detector misplacement tolerance along the detector axis.

The adaptive lens compensates the optical path difference of the catadioptric lens for the 660 nm wavelength rather than the 532 nm wavelength. The sensor lens with an aperture generates variation signals at different positions and angles between the catadioptric lens and the disc. According to the variation signals of the servo light detected at the central area of the CCD sensor, the feedback signal after calculation actuates the catadioptric lens to the correct position and is angle-related to the disc, as shown in Fig. 4.

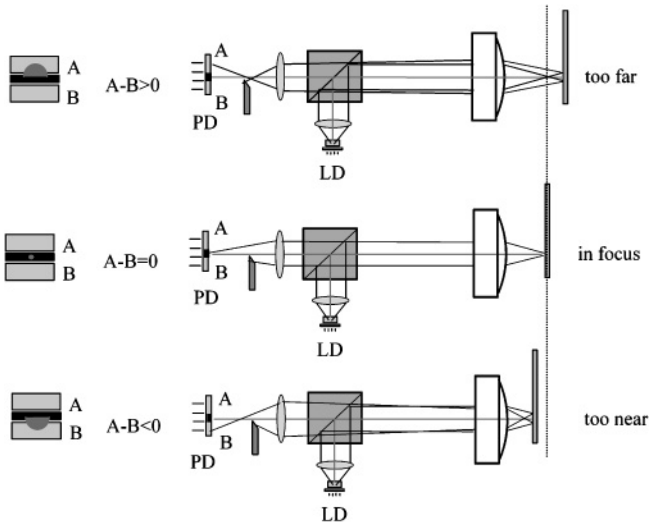

Fig. 3. Pupil obscuration method.

The simulated radii of the spots in the CCD camera of the system are shown in Fig. 4. The focusing S curve can be generated to find the accurate position by computing the radius with the Knife-edge method from CCD. The problem considered here is that of fitting a circle to a set of measured data points specified in terms of their Cartesian coordinates. The least-squares method is used to solve a set of linear equations having more equations than unknown variables by minimizing residual errors. The iteration ends until the results converge (the adjustment approaches zero). The linear case is an adjustment using zero as the initial guess of all parameters.[7,8)]

The lenses are made of Zeonex, as shown in Fig. 5, and the profile of its reflecting surfaces is formed by diamond-turning machining (ULG-100CH). Then the first two surfaces S1 and S2 of the lens are coated with Au for full reflection, as shown in Fig. 4. The second surface S2 is painted black to prevent stray light. The surface profiles of the catadioptric lens are measured using an ultrahigh accurate three-dimensional profilometer (UA3P), as shown in Fig. 6.

This experiment was designed to apply the Knife-edge method in a holographic system with a catadioptric lens, whose surface was patially coated with Au for phase conjugate readout. The least-squares method was used to solve a set of linear equations for the spot size of CCD. Data were obtainted to generate an S curve, which was used in the pupil obscuration method, for a focusing servo. Subsequently, the focusing servo was added to control the system operated in a linear range of ± 0.3 mm, as shown in Fig. 7.

A short-focal-length Fourier-transform-lens system for holographic storage contains a catadioptric Fourier transform lens with a focal length of 31 mm and a central part area for a focusing optical servo. We successfully design the catadioptric Fourier transform lens, which has a surface partially coated with Au and is telecentric in the object plane, for a phase conjugate readout holographic system. The holographic system uses an optical servo method in focusing a direction within the central area of a catadioptric system.

Disc position (mm)	0.4	0.1	0.06	0.02
CCD (Inner circle is airy disc R= 8.67 μm)	163.06 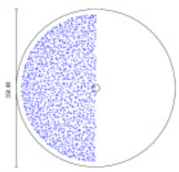	33.6 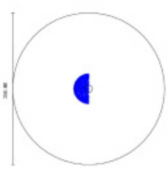	16.47 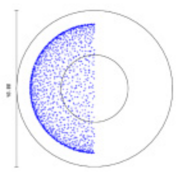	<Airy disc 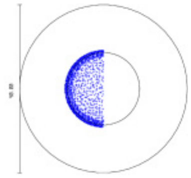
Radius (μm) of outside circle	350	350	40	40
Disc position (mm)	0	-0.03	-0.1	-0.3
CCD (Inner circle is airy disc R= 8.67 μm)	9.97 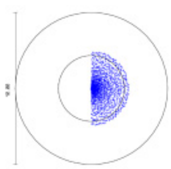	22.84 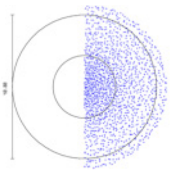	53.3 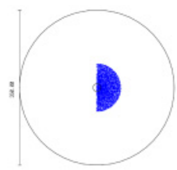	140.63 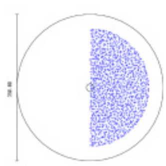
Radius (μm) of outside circle	40	40	350	350

Fig. 4. (Color online) Spot size measurement for shifting disc in focusing direction ($\lambda = 660$ nm).

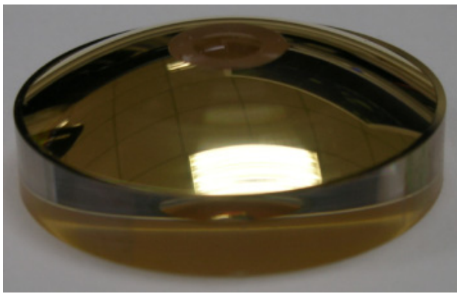

Fig. 5. (Color online) Catadioptric lens.

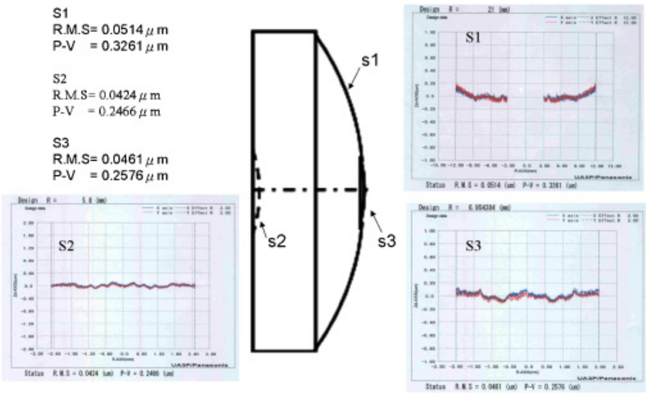

Fig. 6. (Color online) Catadioptric lens measurement.

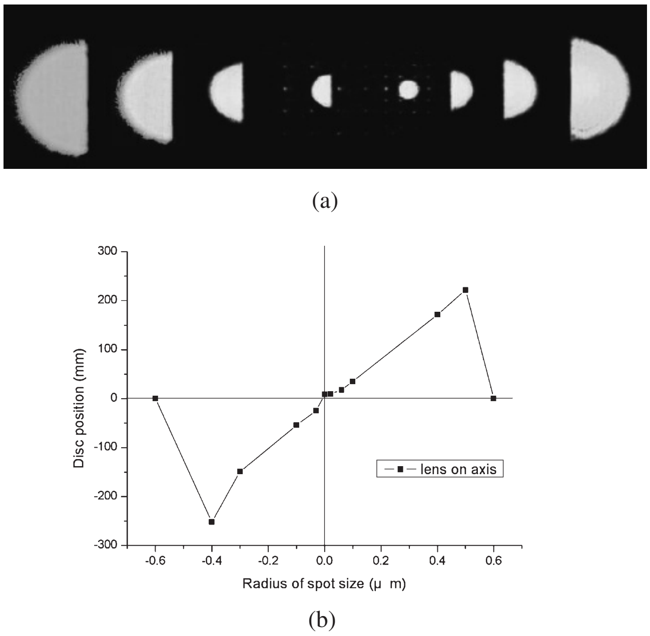

Fig. 7. Spot diameter of CCD measurement and S curve of focus error detection for lens on axis.

Acknowledgements

The authors would like to acknowledge Kuang-Vu Chen for valuable discussion and technical assistance. This work was supported by the National Science Council, Republic of China under Contract No. NSC96-2752-E009-009-PAE.

1) J. F. Heanue, M. M. Bashaw, and L. Hesselink.: Science **265** (1994) 749.
2) S. S. Orlov, W. Phillips, E. Bjornson, Y. Takashima, P. Sundaram, L. Hesselink, R. Okas, D. Kwan, and R. Snyder: Appl. Opt. **43** (2004) 25.
3) J. W. Goodman: *Introduction to Fourier Optics* (McGraw-Hill, New York, 1996) 2nd ed., p. 333.
4) D. R. Shafer: Appl. Opt. **17** (1978) 11.
5) W. J. Smith: *Modern Lens Design* (McGraw-Hill, New York, 2005) 2nd ed., p. 456.
6) Y. S. Lan and C. H. Tien: Jpn. J. Appl. Phys. **46** (2007) 3867.
7) S. G. Nash and A. Sofer: *Linear and Nonlinear Programming* (McGraw-Hill, New York, 1996).
8) P. R. Wolf and C. D. Ghilani: *Adjustment Computations* (Wiley, New York, 1997).